Spectroscopy by frequency-entangled photon pairs

Atsushi Yabushita and Takayoshi Kobayashi

Core Research for Evolutional Science and Technology (CREST), Japan Science and Technology Corporation (JST) and Department of Physics, Graduate School of Science, University of Tokyo, 7-3-1 Hongo, Bunkyo, Tokyo 113-0033, Japan

Quantum spectroscopy was performed using the frequency-entangled broadband photon pairs generated by spontaneous parametric down-conversion. An absorptive sample was placed in front of the idler photon detector, and the frequency of signal photons was resolved by a diffraction grating. The absorption spectrum of the sample was measured by counting the coincidences, and the result is in agreement with the one measured by a conventional spectrophotometer with a classical light source.

I. INTRODUCTION

The polarization entanglement of spatially separated photon pairs, generated by spontaneous parametric down-conversion (SPDC), has been used in a variety of quantum experiments to demonstrate quantum teleportation, entanglement-based quantum cryptography, Bell-inequality violations, and others [1].

These SPDC photon pairs are also entangled in their wave vectors. The entanglement in wave-vector space is used in various experiments, such as quantum imaging [2,3], photonic de Broglie wavelength measurement [4–6], quantum interference [7,8], and quantum lithography [9–11]. It was claimed and experimentally verified that they have higher resolution than the classical limit, which will be used to various applications.

On the other hand, in the case of quantum imaging, the information about the shape of a spatial filter is transferred by entangled photon pairs, therefore it is useful for secure two-dimensional information transfer. Compared with the case using the polarization entanglement, it can send much more information by the entanglement of the wave-vector space taking an advantage of the continuity of the entangled parameter. A protocol for quantum key distribution was proposed based on a system whose dimension is higher than 2 in Ref. [12].

In this paper, a frequency entanglement was used to measure the spectroscopic property of a sample, which can also be used for nonlocal pulse shaping [13]. The state was maximally entangled by using a continuous-wave (cw) pump [14–16]. Focusing the pump on a SPDC crystal by an objective lens, the bandwidth of SPDC was extended. It enabled us to measure the absorption spectrum of a sample in broadband. Various types of spectroscopic measurements were performed utilizing classical light source including sophisticatedly constructed extremely short pulses [17]. However, in the following situations, spectroscopy utilizing the frequency entanglement can be a powerful way to measure the spectroscopic properties of the sample.

One of the situations is the case when it is difficult to analyze frequency of photons transmitted through an absorptive sample. For example, to measure the spectroscopic property of a sample in vacuum ultraviolet (VUV) range, a spectrometer must be settled in a vacuum chamber in case of the conventional VUV spectroscopy, and the spectrometer must be aligned and controlled under the vacuum condition. However, in case of spectroscopy using the frequency-entangled photon pair consists of a VUV photon and a longer wavelength photon (like a visible photon), the VUV photon transmitted thorough the sample is to be detected by the photodetector without capability of energy resolution. Instead the visible photon is to be resolved by a spectrometer in the atmospheric pressure which is easily handled. This is one of the useful features of this method. The method is also useful when the sample is in space and the photons transmitted through the sample are not easy to be resolved by their energy.

Another situation is the case when the spectroscopic property of a fragile sample is to be measured in infrared range. The power of the light source must be very low not to damage the sample, and yet an infrared photodetector is usually so noisy that a signal-to-noise ratio is very low in the measurement using the classical light source. However, when the frequency-entangled photon pairs are used, the coincidence counts are measured, then one of the photons of each photon pair works as a timing gate for the measurement of another photon of the pair which is to be resolved by its energy, and the signal-to-noise ratio is expected to be enhanced substantially. This is another advantage of this method.

The SPDC photon pairs are emitted conically from the point where the pump light is focused on the beta-barium borate (BBO) crystal. Using a parabolic mirror, all SPDC photon pairs in the light cones are collimated without achromatic aberration, and travel to a beam splitter without expanding their beam diameters keeping their polarization entanglement. It is not aimed to use the polarization in this experiment, so signal and idler photons are separated from each other by a polarizing beam splitter which destroys the polarization entanglement. When a nonpolarizing beam splitter is used in place of the polarizing beam splitter, the photon pairs detected at the photon counters have polarization entanglement, which can be used for quantum cryptography [18,19]. Therefore using the polarization entanglement and the frequency entanglement simultaneously, it will become possible to implement wavelength-division multiplexing (WDM), quantum cryptography, or WDM quantum key distribution, which can send much more information compared with the case of polarization-only entanglement.
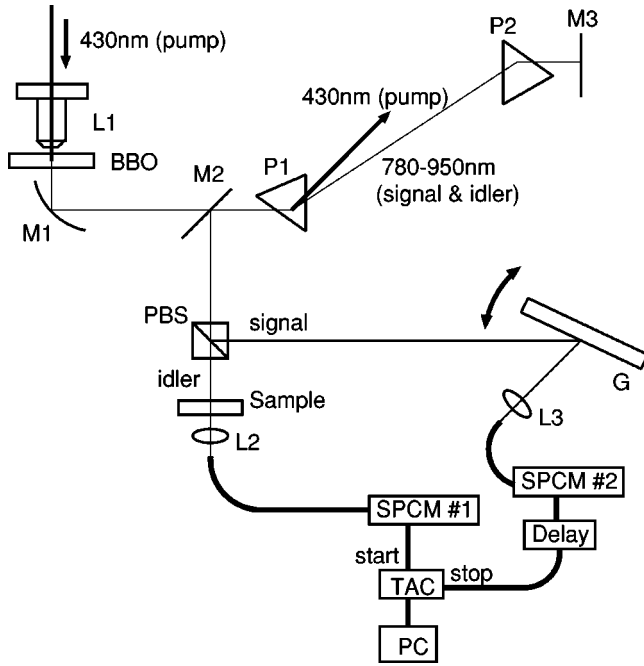
FIG. 1. Experimental setup. Details are given in the text.

II. EXPERIMENT

The schematic drawing of our experimental setup is shown in Fig. 1. Frequency-nondegenerate photon pairs are generated by SPDC in a 1-mm-thick type-II BBO (β-BaB$_2$O$_4$) crystal pumped by the second harmonic light (1.5 mW) of a cw Ti:sapphire laser operated at 859.4 nm. To generate photon pairs by bandwidth extended SPDC, the pump light is focused on the BBO crystal by a microscope objective lens of 8-mm focal length (L1). Generated SPDC photons diversing from the focal waist are collimated by an off-axis parabolic mirror (M) of 25.4-mm focal length. A prism pair (P1,P2) is used to eliminate the remainder of the pump light, which can be a noise source in the experiments. When the light beam passes through the prism pairs, the beam height was lowered by a mirror (M3), and only the SPDC pairs are picked out by another mirror (M2). The signal and idler photons were separated from each other by a polarizing beam splitter (PBS). Vertically polarized photons (signal) are reflected by the PBS, and diffracted by a grating (G) (1400 grooves/mm). Horizontally polarized photons (idler) pass through the PBS and a partially absorptive sample.

A 2.5-mm-thick plate of Nd^{3+}-doped glass was used as a sample. The main absorption transitions in Nd^{3+} around the visible spectral range are from $^4I_{9/2}$ to $^2G_{7/2}(^2G_{5/2})$, $^4F_{7/2}$, $^4F_{5/2}$, and $^4F_{3/2}$, of which peak wavelengths are located at about 580, 750, 810, and 870 nm, respectively. The spectrum of signal light is centered at 840 nm, and it overlaps with the absorption peaks at 810 and 870 nm (see Fig. 2), of which transitions are studied in this paper.

Both signal and idler photons are collimated into fibers by lenses (L2,L3) and then detected by a set of two single-photon counting modules (SPCM: EG&G SPCM-AQR-14). Delaying the electric signal from the SPCM detecting signal
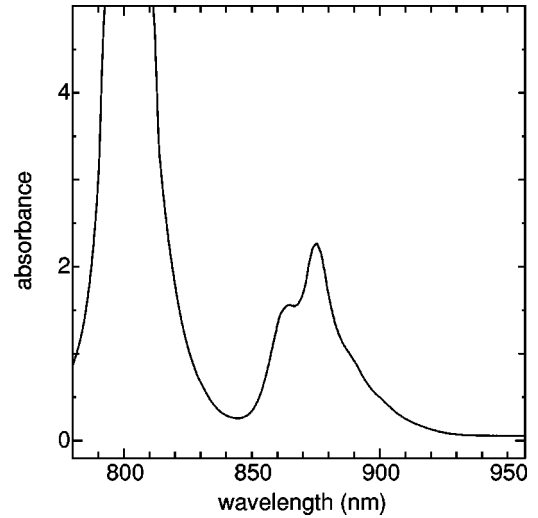
FIG. 2. Absorption spectrum of Nd^{3+}-doped glass.

photons by a nanosecond delay unit (ORTEC 425A), the coincidences are counted by a time-to-amplitude converter/ single-channel analyzer (ORTEC 567) followed by a computer-controlled multichannel pulse-height analyzer (MCA:ORTEC TRUMP-PCI-2k).

III. THEORY

In this paper, we discuss the application of the frequency-entanglement of SPDC photon pairs to absorption spectroscopy. The state of generated SPDC photon pairs can be written as [14–16]

$$|\psi\rangle \propto \int d\omega_s \int d\omega_i \tilde{E}(\omega_s+\omega_i)\Phi_L(\omega_s,\omega_i)|\omega_s\rangle_s|\omega_i\rangle_i, \tag{1}$$

where $|\omega\rangle_j \equiv a_j^\dagger(\omega)|0\rangle$ is a single-photon state whose frequency is ω. $a_j^\dagger(\omega)$ is the photon creation operator for frequency ω photons. Here $j=p$, s, and i indicate the pump, signal, and idler waves, respectively. $\tilde{E}(\omega)$ is the Fourier transform of the classical field of pump laser, and

$$\Phi_L(\omega_s,\omega_i) \propto \text{sinc}[\Delta k(\omega_s,\omega_i)L/2] \tag{2}$$

is the phase-matching function [20], where $\text{sinc}(x)=\sin(x)/x$, with the phase mismatch parameter Δk expressed as

$$\Delta k(\omega_s,\omega_i) = k_s(\omega_s)+k_i(\omega_i)-k_p(\omega_s+\omega_i). \tag{3}$$

As easily seen from Eq. (2), thinner crystals are preferable for the generation of broadband SPDC photon pairs. Generally, in our quantum experiments using SPDC photon pairs, thick crystals as thick as 5 mm are usually used to obtain high SPDC conversion efficiency. However in this paper broadband SPDC photon pairs are indispensable for its spectroscopic measurement, thin crystal of 1-mm thickness is used.

The wavelength resolution of this system is calculated as 4 nm using $d_g\phi_f/2F$, where d_g, ϕ_f, and F are a gap of grating grooves (1/1400 mm), a fiber diameter (125 μm),
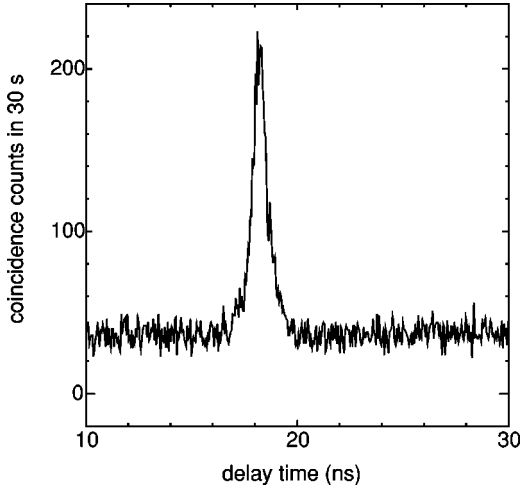
FIG. 3. Coincidence counts accumulated for 30 s when the grating angle is set to diffract center wavelength of signal light.

and a focal length of lens L2 (11 mm), respectively. It is much narrower than the full width of the parametric fluorescence spectrum.

Since a cw laser is being used as a pump, the pump bandwidth is also much narrower than the width of the parametric fluorescence spectrum. It forces the sum of signal and idler frequency to be equal to the pump frequency as $\omega_p = \omega_s + \omega_i$, and it entangles a SPDC photon pair in its frequency as a signal photon at frequency $\omega_p/2 - \omega$ is generated with an idler photon at frequency $\omega_p/2 + \omega$.

The wavelength resolution of the system and the pump bandwidth are so narrow that, using some approximations, the absorption spectrum of the sample can be easily calculated as [21,22]

$$A(\omega') = -\log_{10}\frac{R_c(\omega_p - \omega')}{R_{c,\text{sample}}(\omega_p - \omega')}, \qquad (4)$$

where $R_{c,\text{sample}}(\omega)$ is a coincidence counting rate when the sample was placed in the idler path, and $R_c(\omega)$ is the one without the sample.

IV. RESULTS AND DISCUSSION

Figure 3 shows coincidence counts accumulated for 30 s without a sample when the grating angle is set to diffract the center wavelength of signal light, and the coincidence counts have a peak at the delay time of 18 ns determined by the delay unit.

Coincidence counts averaged from 5 to 45 ns except between 14 and 22 ns delay is used for the calculation of a background noise. In this paper, coincidence sum counts are obtained by the integration of the coincidence counts during the delay from 14 to 22 ns and by subtracting the background noise.

Rotating the grating around the vertical axis crossing the incident point of the idler beam, coincidence counts are accumulated for 120 s at each step without a sample. The dashed curve in Fig. 4 shows the wavelength dependence of
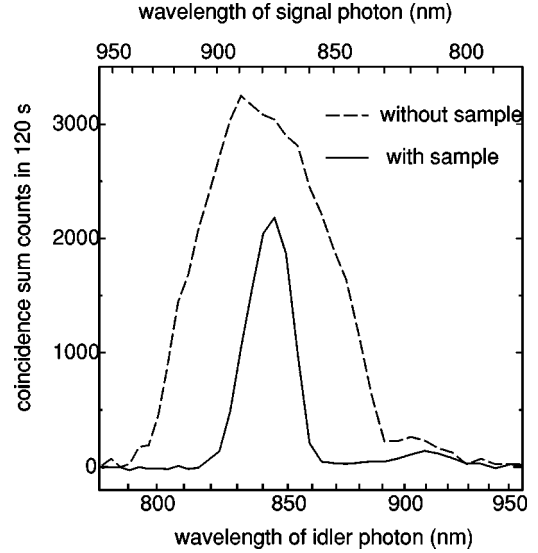

FIG. 4. Coincidence spectrum with the Nd^{3+}-doped glass sample, accumulated scanning a grating angle (solid line) and one without a sample (dashed line).

the sum of coincidence counts at each step (coincidence spectrum). The center wavelengths of the signal and idler are centered at 883 and 840 nm, respectively, and the full widths at half maximum (FWHMs) are 63 and 69 nm, respectively.

Then, rotating the grating, coincidence spectrum was measured with the Nd^{3+}-doped glass sample in the idler light path, accumulating for 120 s at each step (see Fig. 4). The wavelength calibration is performed using a reflection, zeroth-order diffraction, from the grating. Beside the center wavelength of the SPDC light, the glass sample has two absorption peaks at about 810 and 870 nm (see Fig. 2), so the idler photons are absorbed and the coincidence counts are reduced in the spectral ranges.

By dividing the coincidence spectrum without a sample
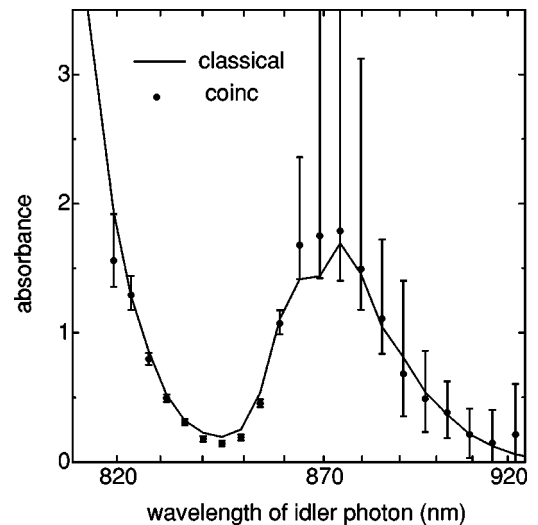

FIG. 5. The absorption spectrum calculated by dividing the coincidence spectrum without a sample by one with the sample. The solid line shows the absorption spectrum measured by a ultraviolet–visible–near-infrared (UV-VIS-NIR) spectrophotometer.

by one with the sample, the absorption spectrum of the sample is calculated, and compared with one measured by a ultraviolet–visible–near-infrared (UV-VIS-NIR) spectrophotometer in Fig. 5. The absorption spectrum determined from the ratio of the coincidence counts fits fairly well with the one measured by the conventional spectrophotometer except in the spectral range from 860 to 880 nm, where the sample absorbance is large and the amount of transmitted photons is so small that the error tends to be substantially large.

V. CONCLUSION

In conclusion, the absorption spectrum of the Nd^{3+}-doped glass plate was measured using an frequency entangled two-photon state generated by spontaneous parametric down-conversion. This method is performed without resolving the frequency of idler photons which transmit through the sample. It is greatly advantageous in the case when the transmitted photons are not easy to be resolved by their energy, like in vacuum ultraviolet range or in space. The method using the frequency-entangled photon pairs has an advantage over the one using classical method, when the spectroscopic property of a fragile sample is analyzed in a spectral range where any low-noise photodetector is not available, like in infrared range. Not to damage fragile samples, the pump light power must be very low, but the photodetector for a infrared range is usually so noisy that it is difficult to measure the characteristics under such situation. However, using the frequency-entangled photon pairs, one of the photons of each pair can be used as a timing gate for the other photon of the pair resolved by its energy. It increases the signal-to-noise ratio, so the measurement becomes much easier than the case using the classical spectroscopy apparatus.

A type-II BBO crystal is used for production of SPDC photon pairs entangled in polarization. All photon pairs in the SPDC light cones are collimated by a parabolic mirror, and travel to a beam splitter. In this experiment, a polarizing beam splitter was used to separate signal and idler photons from each other effectively. However it destroys the polarization entanglement. Using a nonpolarizing beam splitter in place of the polarizing beam splitter, the SPDC photon pairs detected at photon counters have the polarization entanglement besides the frequency entanglement, and it will enable WDM cryptography to be implemented which has an ability to send much more information than the case not using the frequency entanglement.

[1] W. Tittel and G. Weihs, in *Quantum Information and Computation* (Rinton Press, Princeton, NJ, 2001), Vol. 1, pp. 3–56.

[2] Y. Shih, J. Mod. Opt. **49**, 2275 (2002).

[3] T.B. Pittman, Y.H. Shih, D.V. Strekalov, and A.V. Sergienko, Phys. Rev. A **52**, R3429 (1995).

[4] E.J.S. Fonseca, C.H. Monken, and S. Pádua, Phys. Rev. Lett. **82**, 2868 (1999).

[5] J. Jacobson, G. Björk, I. Chuang, and Y. Yamamoto, Phys. Rev. Lett. **74**, 4835 (1995).

[6] K. Edamatsu, R. Shimizu, and T. Itoh, Phys. Rev. Lett. **89**, 213601 (2002).

[7] D.V. Strekalov, A.V. Sergienko, D.N. Klyshko, and Y.H. Shih, Phys. Rev. Lett. **74**, 3600 (1995).

[8] C.K. Hong, Z.Y. Ou, and L. Mandel, Phys. Rev. Lett. **59**, 2044 (1987).

[9] M. D'Angelo, M.V. Chekhova, and Y. Shih, Phys. Rev. Lett. **87**, 013602 (2001).

[10] R. Shimizu, K. Edamatsu, and T. Itoh, Phys. Rev. A **67**, 041805 (2003).

[11] A.N. Boto, P. Kok, D.S. Abrams, S.L. Braunstein, C.P. Williams, and J.P. Dowling, Phys. Rev. Lett. **85**, 2733 (2000).

[12] H. Bechmann-Pasquinucci and W. Tittel, Phys. Rev. A **61**, 062308 (2000).

[13] M. Bellini, F. Marin, S. Viciani, A. Zavatta, and F.T. Arecchi, Phys. Rev. Lett. **90**, 043602 (2003).

[14] V. Giovannetti, L. Maccone, J.H. Shapiro, and F.N.C. Wong, Phys. Rev. Lett. **88**, 183602 (2002).

[15] W.P. Grice and I.A. Walmsley, Phys. Rev. A **56**, 1627 (1997).

[16] M.H. Rubin, D.N. Klyshko, Y.H. Shih, and A.V. Sergienko, Phys. Rev. A **50**, 5122 (1994).

[17] T. Kobayashi, T. Saito, and H. Ohtani, Nature (London) **414**, 531 (2001).

[18] E. Waks, K. Inoue, C. Santori, D. Fattal, J. Vuckovic, G.S. Solomon, and Y. Yamamoto, Nature (London) **420**, 762 (2002).

[19] C.H. Bennett, Phys. Rev. Lett. **68**, 3121 (1992).

[20] A.M. Weiner, IEEE J. Quantum Electron. **19**, 1276 (1983).

[21] A.I. Lvovsky, H. Hansen, T. Aichele, O. Benson, J. Mlynek, and S. Schiller, Phys. Rev. Lett. **87**, 050402 (2001).

[22] T. Aichele, A.I. Lvovsky, and S. Schiller, Eur. Phys. J. D **18**, 237 (2002).